

Image Formation Free Rotation in Triple Pole-Piece Magnetic Lenses

[1]Hussain S. Hasan, [2]Mohammed Jawad Yaseen
[1]Department of Physiology and Medical Physics, College of Medicine, Al-Nahrain University, P.O. Box: 70044, Kadhimiya, Baghdad, Iraq.
e.mail:altai1965@yahoo.com
[2]Department of Physics, College of Education, the University of Mustansiriyah, P.O.Box:46219, Baghdad, Iraq.
e.mail:m1964jy@yahoo.com

ABSTRACT
Present work is mainly concern with the mathematical function, considered to represent the axial magnetic flux density distributions of proposed triple pole-pieces magnetic lenses which is used as rotation free lenses. This function has, in fact, three-optimization parameters. The only important parameter is the bore radius of the lens in the proposed model. This parameter can be affect on the projector properties of the lens, when the other two optimization parameters (maximum value of flux density and lens length) are constants, where the literature survey proved that unaffected on the lens properties. Results have clearly shown that the optimization parameter for current function, have a considerable effect on the lens distortion, lens magnification, and the reconstructed pole-pieces. Furthermore, the results obviously show the excellent ability for converting the form of the chosen mathematical function in order to represent the magnetic field of triple pole-pieces lenses.

Keywords: Electron Optics, Projector Lens, Distortion, Magnification

1. INTRODUCTION

The main fundamental concept of the electron and ion optics is based on the analogy between geometrical light optics and the motion of charged particle beams in electromagnetic fields. The elementary charged particles have the duality nature similar to the light according to De Broglie and Busch discoveries which state that a wave associated with a moving particle and time independent fields (magnetostatic fields) of a solenoid acts on charged particles in a way similar to that of glass lens on light rays. Therefore, in the field of the electron optical instruments electrons or ions used in the imagining processes instead of photons in the optical devises. This means that visible light in optical microscope is replaced by electron beams of varying wavelength depending on the accelerated voltage in the electron microscope. The elementary component in the electron microscope and other electron optical instruments is the electron lens (electrostatic or magnetic lens) which can be defined as any axially symmetric electrostatic or magnetostatic field distribution has a focusing effect on any charged particle beam.

Many investigations have been concerns with the inverse design problems of electrostatic and magnetic electron lenses by using some objective functions, for more details see [1].

The present work deals with the second approach including evaluation of the projector focal properties and determined the pole-piece profiles of the symmetrical magnetic field distributions by using a new mathematical target function.

2. MATHEMATICAL MODEL

In general, synthesis (inverse design) optimization procedure in the field of electron and ion optics contrary on the analytical treatments begins with a specific target function to represent the axial magnetic field, potential or trajectory distributions along the optical axis of the electron lens. This technique has been depended in all previous investigations of symmetrical and asymmetrical double pole-piece magnetic electron lenses. However, this procedure starts with any one of the mentioned target functions, where begins with a specific target function to represent the axial magnetic field in current study. The proposed mathematical model has been introduced.

$$B_z(z) = \frac{B_{max} r_b^{\,4}}{\left(z^2 + r_b^{\,2}\right)^2} \tag{1}$$

Where B_{max} is the maximum value of axial flux density, z is the axial distance on the optical axis, and r_b is the bore radius of the lens. Also, it is important to investigate the scalar magnetic potential V according to the relation;

$$B_z = -\mu_o \, gradV \tag{2}$$

Where μ_o is the magnetic space permeability and equal to $4\pi x10^{-7}H.m^{-1}$ .By using the analytical solution of Laplace's equation, the shape of the pole piece that would produce the desired field can be determined. For axially symmetric systems the electrostatic or magnetic scalar potential V(r,z) can be calculated from the axial distribution of the same potential V(z) by the following series expansion [2]-[3].

$$V(R_p, z) = \sum_{k=0}^{\infty} \frac{(-1)^k}{(k!)^2} \left(\frac{R_p}{2} \right)^{2k} \frac{d^{2k}V(z)}{dz^{2k}} \tag{3}$$

Where R_p is the radial height of the pole-piece, V_P is the potential value at the pole-piece surface, which is equivalent to half of the lens excitation NI and $V_z^{''}$ is the second derivative of the magnetic scalar potential with respect to the z-coordinate. By taking the first two terms of equation (3) under consideration, the equipotential surfaces are given by the formula [4]-[5].

$$R_P(z) = 2\left[\frac{V(z) - V_P}{V''(z)} \right]^{\frac{1}{2}} \tag{4}$$

It is easy then to use equation (1) to assigning the imaging magnetic field distribution along the optical axis $z_1 \leq z \leq z_2$. By using the magnetic field determinations, the one can calculate the electron beam trajectory r(z) and its correspondence departure $r'(z)$ with optical axis z. Typically, this task can be achieved by solving the paraxial ray equation given by the following expression [6]-[7].

$$r'' + \frac{\eta}{8V_r} B_z^2(z) r = 0 \tag{5}$$

Where η represents the charge-to-mass quotient, V_r is the relativistically corrected accelerating voltage and r is the height of the electron beam trajectory from the optical axis.
In the present work the radial D_r and spiral D_s distortion coefficients can be determined by using the following integrals [6].

$$D_r = \left(\frac{\eta}{128V_r} \right) \int_{z_1}^{z_2} \left[\left(\frac{3\eta}{V_r} B_z^2 + 8B_z'^2 \right) r_\alpha r_\gamma^3 - 4B_z^2 (r_\gamma'^2 r_\alpha r_\gamma + r_\gamma' r_\alpha^2 r_\alpha') \right] dz \tag{6}$$

$$D_S = \int_{z_1}^{z_2} \left[\frac{3}{128} \left(\frac{\eta}{V_r} \right)^{3/2} r_\alpha^2 B_z^3 + \frac{1}{16} \left(\frac{\eta}{V_r} \right)^{1/2} r_\alpha'^2 B_z \right] dz \tag{7}$$

Where r_α and r_γ are two linearly independent solutions of the paraxial-ray equation (5). The limits of integration are the two terminals points' z_1 and z_2 of the magnetic field. The magnification of doublet projector lenses determine at first and second loop, using the formula [8].

$$M = \frac{\ell L}{(F_P)_{min}^2} \tag{8}$$

Where M is the magnification of the doublet projector lens, ℓ is the distance between the center of two peak of the field (here in proposed lens ℓ = 20 mm), L is the distance between the face of the second lens and the screen (in current work imposed L=35 mm), and $(F_P)_{min}$ is the minimum projector focal length.

3. RESLUTS AND DISCUSSION

Obviously equation (1) implied three optimization parameters namely B_{max}, z, and r_b (in current work kept B_{max}, and z constants). In order to clarify the effect of varying the optimization parameter r_b , five values have been chosen (r_b = 1, 2, 3, 4, and 5mm) and the optical axis chosen to be 40mm. The axial magnetic flux density distribution (B_z) should be compute it according to equation (1) for various values of bore radius and plot it as a function of axial distance (z) as shown in figure 1. From figure 1 one notice the increasing values of r_b with remain B_{max} constant leads to increasing the area under magnetic field curve, i.e. increasing the lens excitation NI.

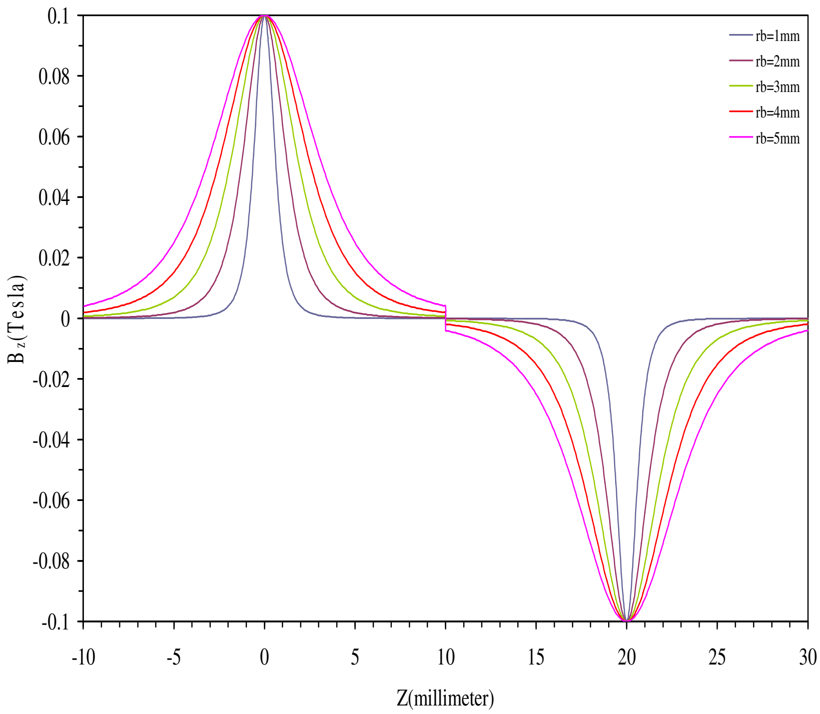

Figure 1. The axial magnetic field distributions of a doublet lens at r_b = (1, 2, 3, 4, and 5mm) and L=40mm.

The magnetic scalar potential V(z) distribution should be computed from equation (2) , as shown in figure 2. According to figure (2), can shows the V(z) distribution curves correspond to each chosen value for r_b , and seen that whenever r_b increases, the gradient of V(z) with optical axis increases too. However, this means, directly, the extension of $B_z(z)$ distribution, along the optical axis will be excess as shown in figure 1.

The total reconstructed pole-piece profiles that capable to produce each V(z) distribution, correspond to different values of r_b , are plotted in figure 3. It can be seen that the parameter r_b has an important effect on these shapes, which may due to the variance in $V''(z)$ distributions along the optical axis when r_b varies.

The net effect of the imaging field on the beam trajectory shown in figure 4 is therefore, described as a function of optical axis for various values of r_b leads to out parallel beams, and that is mean truth behavior due to using this lenses with projector role (i.e. infinite operation mode).

The minimum projector focal length F_{pmin} at first and second loop as a function of the bore radius r_b is shown in figure 5. It should be mentioned that, with increase the values of r_b , at first loop F_{pmin} kept constant, but in second loop is decreased.

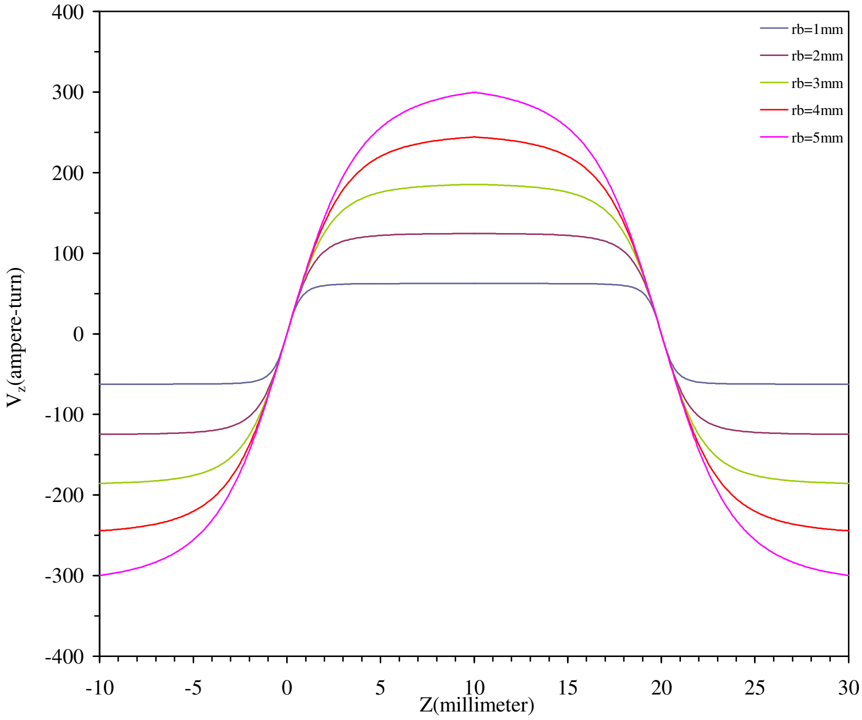

Figure 2. The axial magnetic scalar potential of a doublet lens at r_b = (1, 2, 3, 4, and 5mm) and L=40mm.

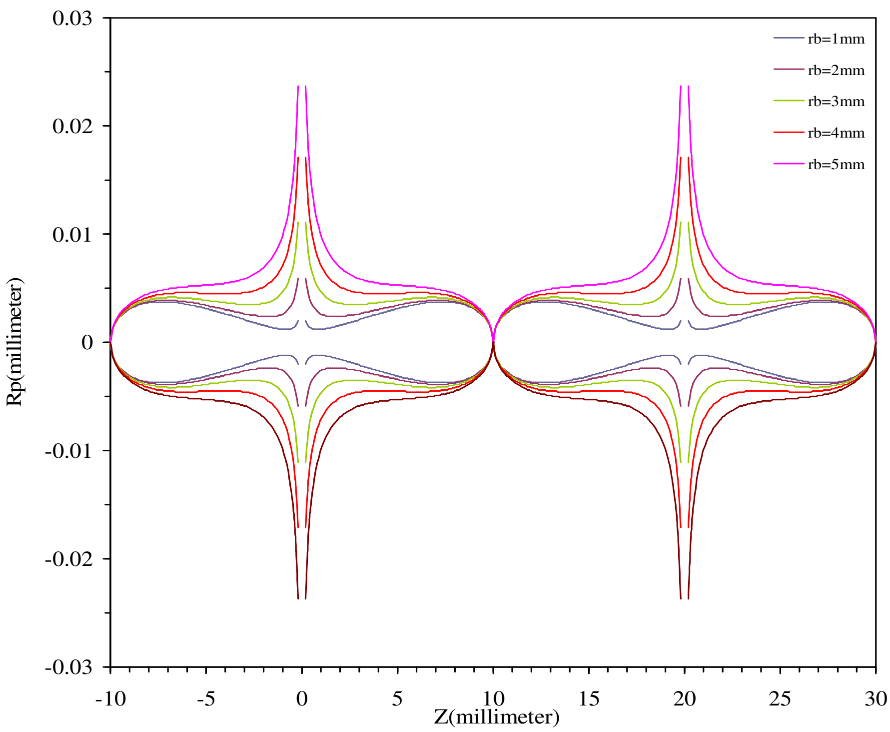

Figure 3. The total reconstructed pole-piece shapes at different values of r_b.

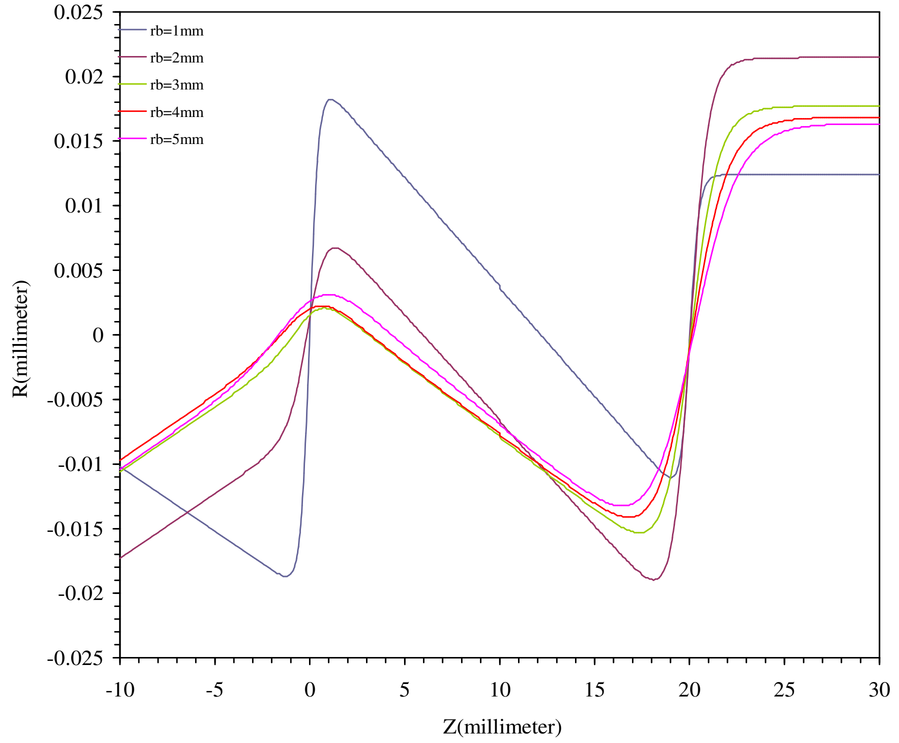

Figure 4. The electron beam trajectory along optical axis at different values of r_b.

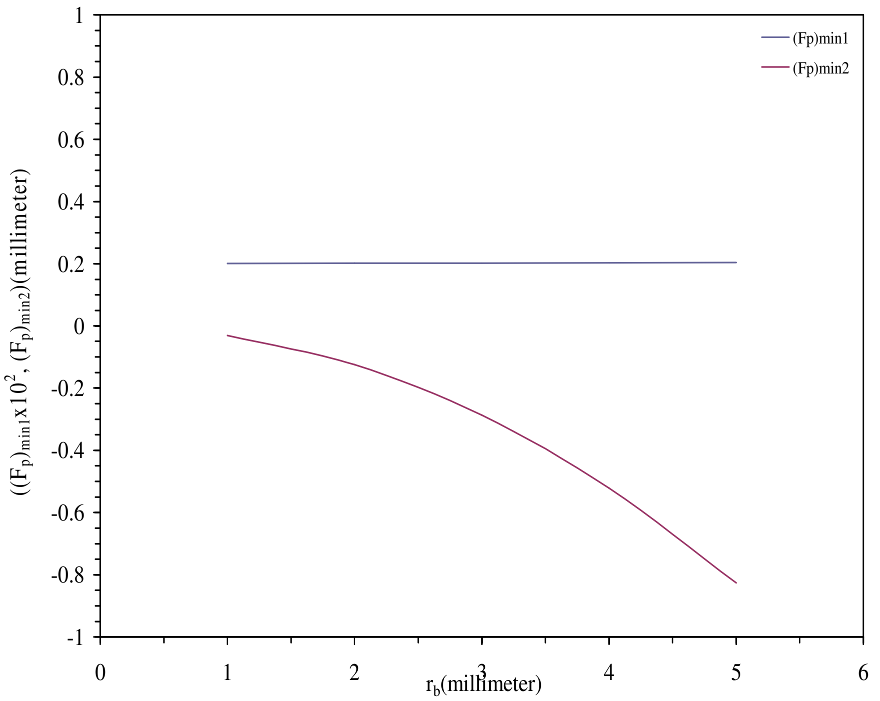

Figure 5. The minimum projector focal length $(F_p)_{min}$ at first and second loop, as a function of r_b.

Figure (6) shows the radial distortion coefficients, D_{r1} in the case of $(F_p)_{min1}$ and D_{r2} in the case of $(F_p)_{min2}$ at first and second loop respectively, at different values of bore radius r_b . It should be mentioned that, when increase the values of r_b , the values of D_{r1} and D_{r2} are sharply decreasing (in low values of r_b<2mm), then stay slight variation for r_b>2mm.

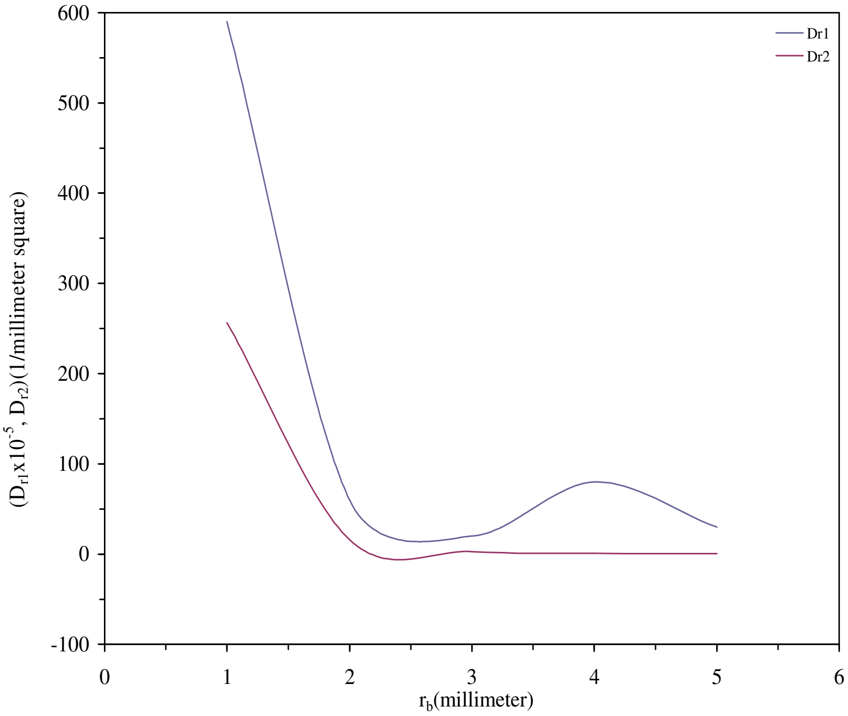

Figure 6. The radial distortion coefficients D_{r1} and D_{r2} at first and second loop as a function of r_b , in the cases of $(F_p)_{min1}$ and $(F_p)_{min2}$ respectively.

The values of spiral distortion coefficients, D_{s1} in the case of $(F_p)_{min1}$ and D_{s2} in the case of $(F_p)_{min2}$ at first and second loop respectively, represented at different values of bore radius r_b , as shown in figure 7. It should be mentioned that when increase the values of r_b , the values of D_{r2} are sharply decreasing (in low values of r_b < 2 mm), then stay slight variation for r_b>2mm, while the values of D_{r1} are increasing from negative values toward x-axis (zeros distortion).

The main two defects, radial D_r and spiral D_s distortions, which the projector lenses suffer from it at the minimum projector focal length $(F_p)_{min}$ in addition to $(F_p)_{min}$ at first and second loop as a function of the excitation parameter $NI/Vr^{1/2}$ as shown in figures 8 and 9 respectively.

From figure 8, it should be mentioned that all of $(F_p)_{min1}$ at first loop kept constant approximately at 20 mm, the values of D_{r1} drop with increasing the values of $NI/Vr^{1/2}$, while the values of D_{s1} increase from negative values approaching to zero, with increasing the values of $NI/Vr^{1/2}$.

From figure 9, the one can see there is a slow decrement in straight line represented the values of F_{pmin2} at second loop, a sharp increase in D_{s2} , while there is a slight decreasing happen in D_{r2} values, all of these happened with increase the values of $NI/Vr^{1/2}$.

The values of half width w , air gap width s , and excitation parameter NI (area under field curve) increasing linearly with increasing the bore radius r_b , as shown in figure 10.

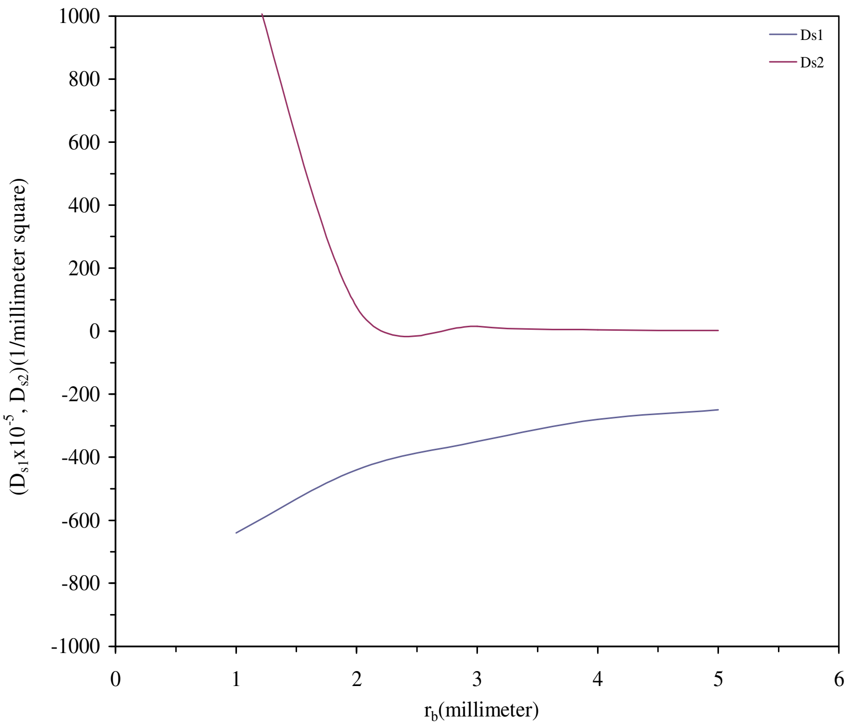

Figure 7. The spiral distortion coefficients D_{s1} and D_{s2} at first and second loop as a function of r_b , in the cases of F_{pmin1} and F_{pmin2} respectively.

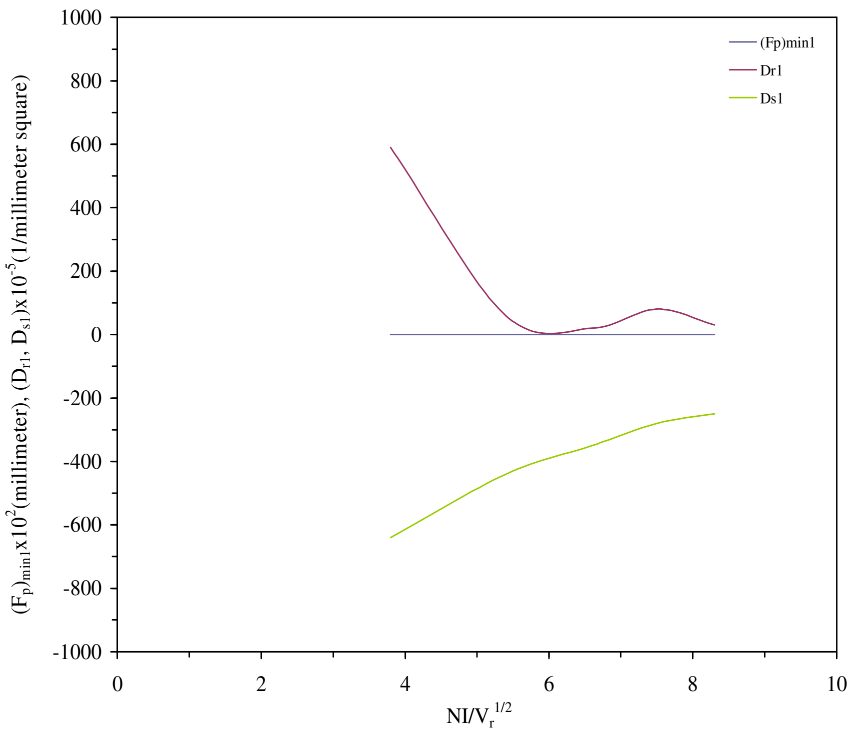

Figure 8. The radial distortion coefficient D_{r1} , and spiral distortion coefficients D_{s1} in the first loop at minimum projector focal length F_{pmin1}, in addition to F_{pmin1} as a function of $NI/V_r^{1/2}$.

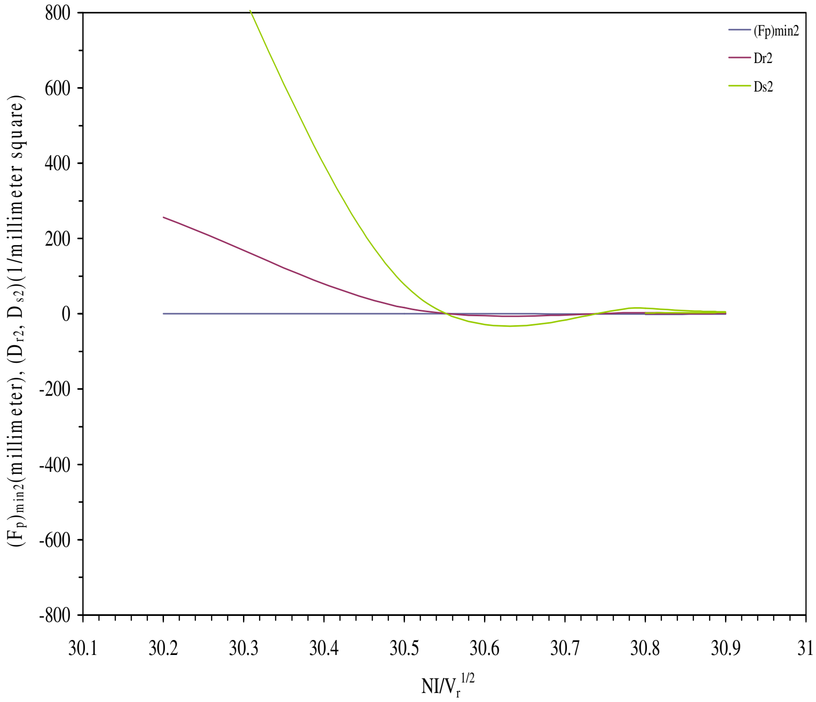

Figure 9. The radial distortion coefficient D_{r2} , and spiral distortion coefficient D_{s2} in the second loop at minimum projector focal length F_{pmin2}, in addition to F_{pmin2} as a function of $NI/V_r^{1/2}$.

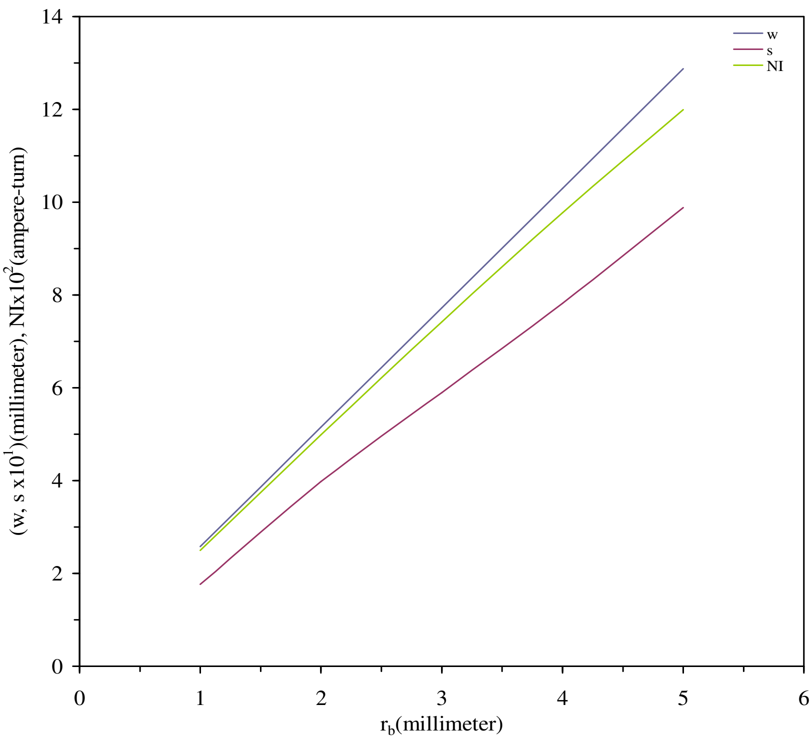

Figure 10. The half-width w, air gap-width s, and excitation parameter NI as a function of r_b.

The magnification of the projector lens, computed from the equation (8) at the first loop M_1, and second loop M_2 for the various values of bore radius r_b . These values represented in figure (11), thus, the one can see the constant values (approximately) of M_1 about 1.7x as a function of r_b , while there is a sharp decreasing happen in M_2 values from hundred thousand times to single thousand times during 2mm from r_b values.

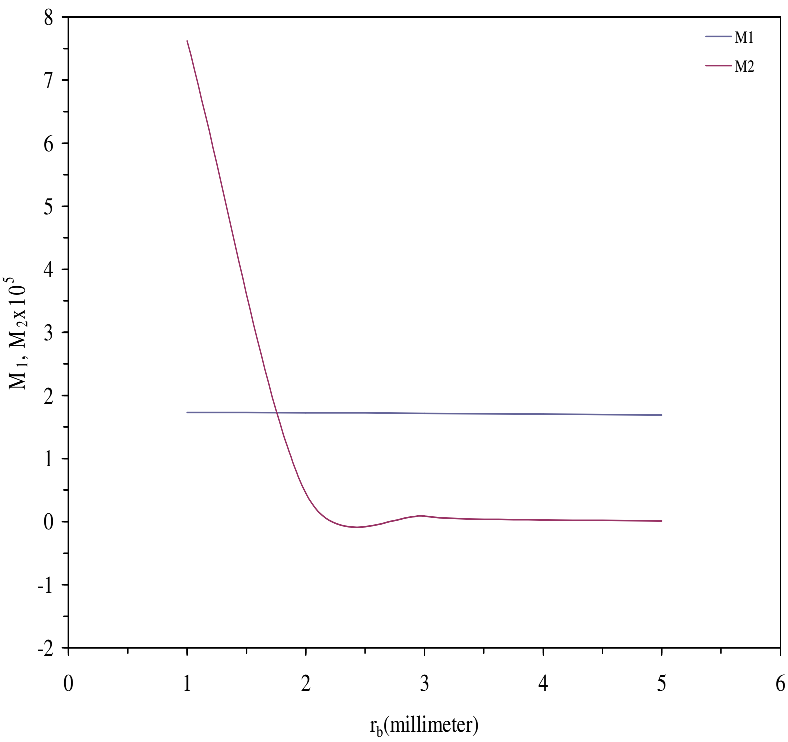

Figure 11. The magnification of the proposed projector lens at first and second loop as a function of r_b.

4. CONCLUSIONS

According to the previous results, several remarks can be stated. The most important of them is that, the mathematical nature of a model which is used to approximate the magnetic field plays an important role to specify its optical properties. In that sense one may replacing the conventional investigation of a magnetic lens by a carful choice of mathematical model to approximate imaging field distribution.

When uses any analytical target function to represent any axial function, such as the magnetic flux density distribution or the scalar magnetic potential or electron beam path ... etc., must take into account that the magnetic field (magnetic flux density distribution) is equal to zero or close to it at the ends (terminals) of optical axis. Otherwise, the part of the excitation will be losing and thus will increase the margin of error in the calculations and cannot get reliable results.

According to the results of the present work one may noticed that, the proposed lens have the same magnification (same minimum focal projector lens), regardless of the bore diameter values in the first loop. While decrease the magnification (increase the minimum focal projector lens) with increase the bore diameter values in the second loop.

The net effect of the imaging field on the beam trajectory leads to out parallel beams, and that is mean truth behavior due to using this lenses with projector role (i.e. infinite operation mode).

The proposed lens have low values of radial and spiral distortion coefficients for values of bore radius greater than 2 mm at minimum focal projector lens in the case of first and second loop.

Effect of decrease the bore radius leads to decrease each of half width of magnetic field, air gap width, and excitation parameter. Thus, this means improve the lens properties regardless of the magnetic flux density especially that required the use of the lens as free rotation - projector lens.

REFRENCES

[1] H. N. Al-Obaidi, A. H. Al-Batat, H. S. Al-Dolami, "synthesis of Symmetrical double pole-piece Magnetic Lens By Means of a Conventional Parameters Function, " Journal of college of Education the University of Mustansiriyah, V(1), pp.454-464, 2009.

[2] M.Szilagyi, "Reconstruction of Electrodes and Pole-pieces from Optimized Axial Field distributions of Electron and Ion Optics Systems, " Appl. Phys.Lett, V(45), pp.499-501, 1984.

[3] M.J. Yaseen, The Objective Properties of the Projector Magnetic Lenses , "Journal of (IJETTCS),V(2), Issue 6, pp.54-59, November-December 2013.
[4] M. Szilagyi, "Electron and ion optics," Plenum Press New York and London, 1988.
[5] M.J. Yaseen, "Projector Properties of the Magnetic Lens Depending on Some Physical and Geometrical Parameters, "Journal of (IJAIEM),V(2), Issue 9, pp.195-202, September 2013.
[6] A. B. El-Kareh, J .C .J. El-Kareh, "Electron beams, lenses, and optics," (Academic Press), 1970.
[7] A.H. H. Al-Batat, "Modeling and Design For Objective Charged Particle Lens,"Journal of (IJAIEM),V(2), Issue 10, pp.25-32, Septmber 2013.
[8] S. M. Juma, "Rotation Free Magnetic Electron Lenses," Ph.D. Thesis, University of Aston, Birmingham, 1975, England, UK.